Egypt. J. Chem. **Vol 63**, No 12, 4805-4819 (2020)

Egyptian Journal of Chemistry

http://ejchem.journals.ekb.eg/

Treatment of petroleum refinery wastewater by electro-Fenton process using porous graphite electrodes

Ahmad S. Fahem [a], Ali H. Abbar [a,b]

[a] *Department of Chemical Engineering, College of Engineering, University of Al-Qadisiyah, AL-Qadisiyah, Iraq*

[b] *Department of Biochemical Engineering, Al-Khwarizmi College of Engineering, University of Baghdad, Baghdad, Iraq*

Abstract

The present paper deals with the treatment of wastewaters generated from Al-Dewaniya petroleum refinery plant by Electro-Fenton process in a batch electrochemical reactor using porous graphite as anode and cathode materials. Effects of operating factors such as current density (5-25mA/cm^2), $FeSO_4$ concentration (0.1-0.7mM), NaCl addition (0-2g/l), and time (15–45min) on the efficiency of the chemical oxygen demand (COD) removal were studied. The results revealed that $FeSO_4$ concentration has the main effect on the efficiency of COD removal confirming that the Electro-Fenton process was governed by reaction conditions in the bulk of solution between ferrous ions and H_2O_2 not upon the electrochemical reactions on the surface of electrodes. Parametric optimization was carried out using response surface methodology (RSM) combined with Box–Behnken Design (BBD) to maximize the removal of COD. Under optimized operating conditions: $FeSO_4$ concentration (0.7mM), current density (25 A/cm^2), and time (45 min) with no addition of NaCl, the removal efficiency of COD was found to be 95.9% with an energy consumption of 8.921kWh/kg COD.

Keywords: petroleum refinery wastewater; Electro-Fenton process; porous graphite; Response surface methodology; COD removal**.**

1. Introduction

In Petroleum refinery process, crude oil converts into its main fractions using physical, thermal, and chemical separation stages then these fractions are further handled via a series of other conversion and separation steps into final products like gasoline, liquefied petroleum gas (LPG), , diesel fuels, kerosene, lubrication oils and many others. For the purpose of getting these products, large quantity of fresh water is utilized for refinery processes, mainly for hydro-treating, distillation, desalting and cooling systems [1]. Nearby 80-90 % of fresh water used in petroleum refinery process convert into wastewaters. During the production stage in the oil refinery processing, the amount of water utilized in this stage was found to be in the range from 0.4 to 1.6 times the amount (volume) of processed oil as reported by Coelho et al. [2]. In this case, the wastewater generated from the oil refinery processing, if not treated, may lead to severe damage to the environment.

The type and concentration of the components involved in the generated wastewaters are based on the type of oils, mode of manufacturing, and process configuration. The polluted wastewater generated by refineries contain COD concentration of nearly 300–600 mg/L; phenol concentration of 20–200 mg/L; benzene concentration of 1–100 mg/L; heavy metals with concentrations as chrome (0.1–100 mg/L), as lead (0.2–10 mg/L), and other contaminants [3]. Direct discharge of these wastewaters could lead to essential pollution problems for the environment due to the high content of polycyclic aromatic compounds that have very toxic effects on the environment since they have the ability to be existed in the environment for a long time. Therefore, it should be treated these effluents before discharging [4].

The traditional methods used for treating of these wastewaters are physical, mechanical, and chemical, usually accompanying with biological treatment. The traditional treatments involve gravitational or centrifugation separations, adsorption with activated carbon, application of coagulants, filtration, flotation, and among others [5,6]. These traditional methods be able to remove solids and emulsified oil as well as free oil in suspension from the wastewater, besides to decreasing

*Corresponding author e-mail: ali.abbar@kecbu.uobaghdad. edu.iq; (Ali H. Abbar).
Receive Date: 17 April 2020, Revise Date: 18 May 2020, Accept Date: 01 June 2020
DOI: 10.21608/EJCHEM.2020.28148.2592

BOD that accompanying with the treatment by biological process. However, using the biological process is insufficient when very toxic recalcitrant pollutants are existed in wastewaters, such as the aromatic fraction from the dissolved organic compounds. Moreover, these traditional methods have shown numerous operational problems like energy consumption, partial degradation of the effluent, secondary phase's generation, and toxic intermediates production that impose extra cost in the process. In this case, innovative methods should be applied to remove these toxic pollutants[7,8].

Advanced oxidation processes (AOPs) are significant treatment methods for active degrading of refractory organic pollutants via oxidation by hydroxyl radicals ($OH^{\bullet}$). Among AOPs, Fenton method is very interesting process due to its high efficiency, low cost, simplicity, and their reagents (hydrogen peroxide and ferrous ion) being non-hazardous[9,10]. In the course of the Fenton process, hydrogen peroxide (H_2O_2) is catalyzed by ferrous ion (Fe^{+2}) to generate $OH^{\bullet}$, which is a highly strong and reactive oxidizing reagent that has ability to react with most of organic materials having C-C and C-H bonds. Fenton's reagents have the ability to eliminate organic pollutants under normal pressure and temperature conditions and permits high depuration with comparatively cheap and plentiful resources. Fenton process is considered as one of the most attractive AOPs that was used in various treatments of water and wastewater, biogeochemistry, atmospheric processes, and biomedical systems [11]. However, in conventional Fenton-based systems, few challenges were observed such as rapid depletion of catalysts, transition and storage of highly concentrated H_2O_2, producing and further disposing of generated iron sludge [12,13]. Therefore, developing new methods should be applied to overcome these drawbacks while maintaining the Fenton process has the same strong oxidation efficiency.

Electro-Fenton process has been introduced as a new modification to the traditional Fenton process for the elimination of organic contaminants. In this process, pollutants are eliminates by Fenton's reagents accompanied with anodic oxidation on the surface of anode. Anodic oxidation alone is not sufficient to eliminate most aromatic contaminants as a result of formation of refractory carboxylic acids, [14]. However, generation of $OH^{\bullet}$ can assist electro-Fenton process to arrive a remarkable efficiency of organic pollutants removal. In comparison with traditional Fenton process, electro-Fenton process, doesn't required the transportation and storing of external H_2O_2 since H_2O_2 is produced in situ, [15] and therefore it is an environmentally friendly process due to the reducing in the usage of chemicals.

In electro-Fenton process, H_2O_2 is formed in situ by reduction of O_2 on the cathode via the passing of an electric current then it react with the dissolved Fe^{2+}. Besides, no secondary pollutants could be created in the overall process due to the existing of catalytic cycle with Fe^{3+} species in the medium that return to $Fe^{2+}$by the direct reduction of Fe^{3+}on the cathode or by different reduction process that involve H_2O_2 or organic intermediate radicals. Therefore, the required quantity of ferrous iron (II) in electro-Fenton is lower than that used in traditional Fenton method [16]. In the anodic oxidation, organic molecules are converted into CO_2 and water due to their reaction with $HO^{\bullet}$ radicals which are produced via direct oxidation of water [17]. In the electro-Fenton process, organic contaminants are eliminated by the action of Fenton's reaction (Eq.1) in the bulk. Besides, it could be removed by anodic oxidation at surface of anode (M) when high oxygen overvoltage anodes are used, like Pt, dimensionally stable anode (DSA), and BDD anode (Eq.2) [18]. H_2O_2 and Fe^{2+} can be continuously produced by simultaneous electrochemical reduction of O_2 and Fe^{3+} (Eqs.3 and 4) respectively on the cathode surface [19,20].

$$Fe^{+2} + H_2O_2 \rightarrow Fe^{+3} + OH^- + OH^{\bullet} \quad (1)$$

$$M(H_2O) \rightarrow M(OH^{\bullet}) + H^+ + e^- \quad (2)$$

$$O_2 + 2H^+ + 2e^- \rightarrow H_2O_2 \quad (3)$$

$$Fe^{+3} + e^- \rightarrow Fe^{+2} \quad (4)$$

The choice of electrode materials is a vital step in the electro-Fenton process. Suitable anodic materials can avoid potential deterioration of electrodes, and high oxygen overvoltage anode can powerfully generate more hydroxyl radicals to improve the efficiency of treatment [21]. Platinum (Pt) is powerful for using as a material of anode in the electrochemical processes because of its high stability and excellent conductivity [9]. However, its use is limited due to its high cost. To overcome this problem, platinized anodes which is formed by plating certain amount of platinum on appropriate metallic substrates, have been used in several electro-Fenton processes and could accomplish similar results as platinum anodes. For example, platinized titanium (Ti/Pt) [22] and Pt-coated steel electrodes [23] have been utilized in early researches. However, their costs is still high making them inappropriate for useful applications. Boron-doped diamond (BDD) is an appropriate anodic material to be used in electrochemical applications. BDD exhibits lower detection limit as well as higher sensitivity because of its wide potential window as well as low background currents in aqueous solutions. For many years, BDD has been used as an anode [24], or both anode and cathode [25]. BDD can produce higher amount of $OH^{\bullet}$ in comparison with Pt electrodes. Also it could completely remove aromatic and unsaturated compounds, however, its effective use for wastewater treatment is still limited by its high cost [26]. Other kinds of anodes utilized in electro-Fenton processes involve titanium coated with RuO_2/IrO_2 (DSA) [27], carbon felts [28], graphite [29] and carbon nanotube (CNT) [30].

Selecting of suitable cathodic materials can straight enhance the efficiency of electro-Fenton by endorsing the productivity of H_2O_2. The dissolved oxygen converts into H_2O_2 either through a 2- electron oxygen reduction reaction (Eq. 5) or by a 4-electron oxygen reduction reaction (Eq. 6). Therefore, the activities of oxygen reduction reaction are based on cathodic materials [20] .

$$O_2 + 2H^+ + 2e^- \rightarrow H_2O_2 \quad (5)$$

$$O_2 + 4e^- + 4H^+ \rightarrow 2H_2O \quad (6)$$

The appropriate nature of cathode can prohibit 4-electron oxygen reduction reaction to maximize the producing of H_2O_2 and the efficiency of electro-Fenton process. The

porous structure of the cathode surface can affect the oxygen mass transfer rate as well as the areas for H_2O_2 generation [28]. Carbon-based materials are usually utilized as cathodic materials for electro-Fenton process due to low catalytic activity for H_2O_2 decomposition, their suitable electrochemical properties towards COD reduction, and high hydrogen overvoltage [31]. Formerly, carbon-based cathode materials which have been used for H_2O_2 generation involve carbon felts [24,28], reticulated vitreous carbon [32], carbon nanotube (CNT) [30], activated carbon fiber [33], graphite rod [34], graphite felt [31], and graphite plates [16].

Few works have been documented that graphite can be used as cathode and anode at the same time in the electro-Fenton process [16, 35,36,37,38&39]. This system has numerous benefits over other electro-Fenton systems. When two dissimilar materials are utilized as electrodes, a layer of anode particles will be formed on the cathode which may effect on the electro-Fenton process efficiency. However, in the case of graphite–graphite electro-Fenton system, the new graphite layer on cathode will improve the system efficiency and will not effect on the system homogeneity [16]. Most of these works reported that graphite–graphite electro-Fenton system is an efficient process for degradation of different wastewaters. Therefore, the aim of the present research is to examine the efficiency of the porous graphite– porous graphite electro-Fenton process for the treatment of wastewater generated from Al-Dewaniya petroleum refinery plant and to optimize the operating factors by using Box-Behnken design (BBD). Quadratic model has been developed in terms of input parameters such as current density, $FeSO_4$ concentration, NaCl concentration, and time by performing the experiments based on design matrix generated by using response surface methodology (RSM). No previous works have been conducted on the optimization of petroleum refinery wastewater using porous graphite– porous graphite electro-Fenton process.

2. Experimental work

Petroleum refinery effluent samples were provided by Al-Dewaniya petroleum refinery plant. Sample (40L) was collected from the feeding tank to the biological treatment unit and stored in closed containers at temperature 4 ºC until use. Characterization of this sample is shown in Table 1. Besides the properties of effluent taken from the settling tank of the final stage of the biological treatment in Al-Dewaniya petroleum refinery plant which were measured by the administration of the plant as well as the permissible limit were mentioned in this table for comparison. The conductivity of raw water is 1.92$mScm^{-1}$ which is low and resulted in increasing the cell potential, therefore supporting electrolyte should be used to increase the conductivity of the solution. Sodium sulfate (Na_2SO_4) at concentration of 0.05 M was used as a supporting electrolyte which gives final conductivity of 11.9 $mScm^{-1}$ which is in the required range to obtain low cell potential [40].

Table 1. Characteristics of the effluents in Al-Dewaniya petroleum refinery plant

Test	feed tank sample	settling tank*	Permissible limit*
COD(mg/l)	560	65	100
pH	6.4	7.5	(6-9.5)
T.D.S. (mg/l)	960	1680	-----
Cl^- (mg/l)	1400	119	100
SO_4(mg/l)	8.835	400	400
Turbidity (NTU)	25.07	6.44	41.3
Conductivity (mS/cm)	1.92	----	-----
Phenol (mg/l)	0.1366	(0.01-0.05)	0.06

*provided by Al-Dewaniya petroleum refinery plant administration

A circular jacketed Perspex glass lab-scale batch electrochemical cell provided with Perspex cover was used for the electro-Fenton treatment experiments. It has inside dimensions (100 mm inside diameter with length of 200 mm and thickness of 5mm) and an active electrolyte volume of 1.0 L. The jacket was made from Perspex and has external dimensions (130mm outside diameter with length of 150 mm). The cover has external dimensions (130 mm outside diameter and thickness of 10mm) and contains two slits for electrodes fixation and holes for inserting the probe of pH-meter, conductivity meter, and sample taking out. A parallel plate configuration was adopted for the electrochemical reactor where porous graphite plates (180 mm × 50 mm × 5 mm) were utilized as anode and cathode. The surface of these electrodes was polished using 600SiC papers then rinsed, sonicated for 15min, and again rinsed with deionized water. The distance between anode and cathode was fixed at 20 mm [41]. Before starting any run, the solution was bubbled with fresh air for 30 min and continuing the bubbling during the run at a rate of 0.5l/min via air compressor (Hailea Electromagnetic Air Compressor ACO-308, China). Bubbling air through solution was achieved by using L-type Perspex tube which was perforated along its horizontal section. A digital d.c. power supply (0–30 V, 0–5 A) Type (UNI-T, UTP3315PF) was used to provide constant current during each experiment. In each run, 1.0L solution was agitated at rotation speed of 500 rpm by using magnetic stirrer to achieve the proper mixing conditions then the required amount of the supporting electrolyte and NaCl (if needed) were added and its pH adjusted using (0.1M)HCl or (0.1M) NaOH to a value of (3)[11]. After that mixing was continued at the same rotation speed during the experiment. All the experiments were carried out at constant temperature 30 ±2 ºC using water bath (Memmert, type: WNB22, Germany). Fig.1 displays the schematic diagram of the electrochemical oxidation experimental setup supported by the required information. The electrolyte pH was measured using a digital pH meter (HNNA Instrument Inc.PH211, Romania). Conductivity and TDS were measured by using (HM digital Inc. model COM-100, Korea). Samples were taken and analyzed to determine the COD and phenol concentration at the end of electrolysis. Solution turbidity was measured by (Jenway-6035, Germany).

SO_4^{-2} and Cl^{-1} was analyzed by using Photo Flex. Series, (WTW model no 14541, Germany).

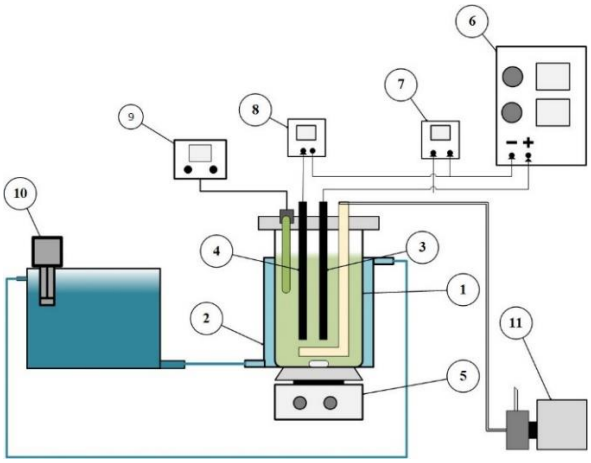

Figure 1. The schematic diagram of the experimental setup: 1) cell body, 2) jacket, 3) porous graphite anode, 4) porous graphite cathode , 5) magnetic stirrer, 6) power supply, 7) voltmeter 8) Ammeter,9) pH-meter10) water bath circulator, 11) air pump**.**

The concentration of total organic compounds in the effluent is expressed in terms of (COD). Amount of COD in petroleum refinery effluents was measured by taken a sample (2ml) of effluent digested with $K_2Cr_2O_7$ as an oxidizing agent for 120 minutes at 150 °C in a COD thermos-reactor (RD125, Lovibond). The digested sample was cooled down to room temperature then analyzed in spectrophotometer (MD200, Lovibond). Phenol was measured by using Method 8047 assigned by Hach Company/Hach Lange GmbH, USA. Measuring of phenol concentration and COD were achieved three times and the average values were taken in this work.

2.1 Characterization of porous graphite electrodes

Porous graphite was used as anode and cathode. It was a rectangular piece UHP graphite electrode with porosity 20-26% used for ARC furnace and supplied by Tokai Carbon Co., Ltd. Its structure was identified by using a X-ray diffractometer (XRD) using Philips Analytical X-Ray B.V. with PC-APD, Diffraction software, Philips xpert, Holland). The XRD was operated at 40 kV and 30 mA with CuKα radiation as the X-ray source, λ=1.54056 Å. The scan step time was 0.5 sec with a step size of 0.02 degrees and a scan range of 10 – 99.99 degrees. The topography of graphite surface was tested using Scanning Electron Microscopy (SEM) using Fesem Tescan Mira3, France. The measurement factors were: AV = 15 kV, bias = 0, spot = 3.0 and HV = 2 kV, bias = 1400 V. The total surface area of graphite was measured by BET method using device (BET Tavana, Iran) provided with software based on micrometrics: MicroActive for TriStar II plus 2.03.

The COD removal efficiency was evaluated based on eq.7 [42]**:**

$$RE\% = \frac{COD_i - COD_f}{COD_i} \times 100 \quad (7)$$

Where RE% stands for the removal efficiency, COD_i represents the initial COD (mg L^{-1}), and COD_f is the final COD (mg L^{-1})

The energy consumption (EC) represents the amount of the consumed energy in the process for a kilogram of COD that requires digesting. EC in (kWh/kg) may be acquired with the use of eq. 8 [43]**:**

$$EC = \frac{E.I.t \times 1000}{(COD_i - COD_f)V} \quad (8)$$

Where EC represents the energy consumption (kWh/kg COD), E represents the applied cell voltage (Volt), t represents the electrolysis time (h), I represents the current (A), V represents the volume of the effluent(L), and COD_f and COD_i represent the final and initial chemical oxygen demand (mg/l).

2.2 Design of experiments

Through application of mathematical and statistical collection, the relationship between a process response and its variables can be determined via adopting RSM [44]. 3-level 4-factor Box–Behnken experimental design was applied in this study to verify and check the factors that influenced on the removal of COD. Current density (X1), Fe SO_4 concentration (X2), NaCl concentration (X3), and time(X4) were taken as process variables, while the COD removal efficiency was taken as a response. The scales of process variables were coded as -1 (low level), 0 (middle or central point) and 1 (high level) [45]. Table 2 illustrates the process parameters with their chosen levels. Box–Behnken develops and improves the designs that needed for getting the suitable quadratic model with the required statistical properties though utilizing only a part of the needed runs for a 3-level factorial design. The number of runs (N) needed for carrying out of Box–Behnken design can be calculated by the following equation [46]:

$$N = 2k(k-1) + cp \quad (9)$$

Where k represents the number of process variables and cp represents the reiterated number of the central point. In this research, twenty seven runs were conducted for evaluating the impacts of the process variables on the COD removal efficiency. Table 3 illustrates the BBD proposed for the present research.

Table 2

Process variables with their level for removal of COD

Process parameters	**range in BBD**		
Coded levels	Low(-1)	Middle(0)	High (+1)
X1- Current density (mA/cm^2)	5	15	25
X2- Fe SO_4(mM)	0.1	0.4	0.7
X3-NaCl (g/l)	0	1	2
X4- Time(min)	15	30	45

Table 3

Box- Behnken experimental design

Run	**Bk.**	**Coded value**				**Real value**			
		x_1	x_2	x_3	x_4	**Current density (mA/cm^2) X1**	**Fe SO4 (mM) X2**	**NaCl (g/l) X3**	**Time (min) X4**
1	1	1	1	0	0	25	0.7	1	30
2	1	1	-1	0	0	25	0.1	1	30
3	1	0	0	-1	-1	15	0.4	0	15
4	1	0	0	0	0	15	0.4	1	30
5	1	0	0	1	-1	15	0.4	2	15
6	1	-1	0	1	0	5	0.4	2	30
7	1	0	0	0	0	15	0.4	1	30
8	1	-1	-1	0	0	5	0.1	1	30
9	1	0	0	1	1	15	0.4	2	45
10	1	0	1	0	1	15	0.7	1	45
11	1	1	0	0	-1	25	0.4	1	15
12	1	0	1	0	-1	15	0.7	1	15
13	1	-1	0	0	-1	5	0.4	1	15
14	1	0	1	-1	0	15	0.7	0	30
15	1	0	0	-1	1	15	0.4	0	45
16	1	0	-1	0	1	15	0.1	1	45
17	1	1	0	1	0	25	0.4	2	30
18	1	-1	0	-1	0	5	0.4	0	30
19	1	1	0	0	1	25	0.4	1	45
20	1	-1	0	0	1	5	0.4	1	45
21	1	0	-1	-1	0	15	0.1	0	30
22	1	0	0	0	0	15	0.4	1	30
23	1	0	1	1	0	15	0.7	2	30
24	1	-1	1	0	0	5	0.7	1	30
25	1	0	-1	1	0	15	0.1	2	30
26	1	0	-1	0	-1	15	0.1	1	15
27	1	1	0	-1	0	25	0.4	0	30

A second order polynomial model can be adopted based on BBD where fitting the interaction terms with the experimental data can be described by the following equation [47]:

$$Y = a_0 + \sum a_i x_i + \sum a_{ii} x_i^2 + \sum a_{ij} x_i x_j \quad (5)$$

Where Y represents the response (RE%), i and j are the index numbers for independed variables, a_0 is intercept term, x_1, x_2 … x_k are the process variables (independent variables) in coded form. a_i is the first-order(linear) main effect, a_{ii} second-order main effect and a_{ij} is the interaction effect. Analysis of variance was performed

then the regression coefficient (R^2) was estimated to confirm the goodness of model fit.

3. Results and discussion

3.1 Statistical analysis

Figure 2 illustrates the XRD results of the porous graphite. It is coincided with the standard graphite structure having a reference code (96-901-2231) (blue) [48]. The graphite structure analysis shows a sharp diffraction peak at 2θ = 26.6255° with C (002) having a d-spacing of 3.34802Å.

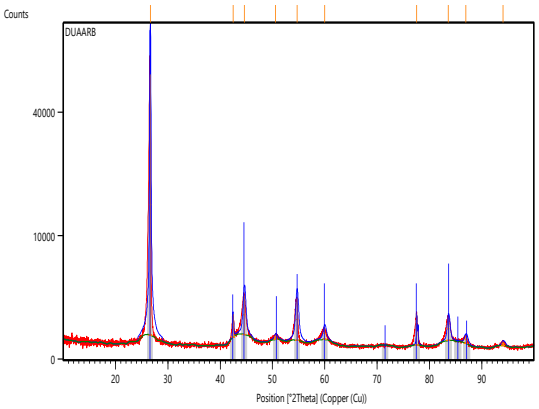

Figure 2. XRD Pattern of porous graphite

The SEM picture of porous graphite anode is shown in Figure 3 with magnification power (7500). It was found that the graphite has high porosity with large pores formed between interconnected structures which is different than the normal rigid graphite that possess smooth non-porous structure. BET surface area of the porous graphite was found to be 22.7509 ± 0.5307 m^2/g.

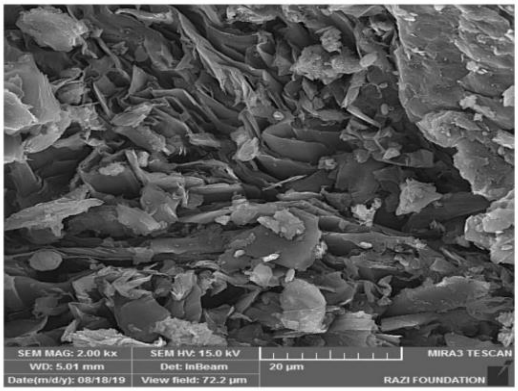

Figure 3. SEM picture of porous graphite

.

3.2 Statistical analysis

For optimizing and investigating the combined impacts of the independent parameters on the COD removal efficiency, twenty seven batch experiments were conducted for various process factors combinations. Table 4 displays the experimental results involving COD removal efficiency (RE %) and energy consumption (EC).

Table 4
Experimental results of BBD for COD removal

Run Order	Blocks	Current Density (mA/cm2)	Fe SO_4 (mM)	NaCl (g/l)	Time (min)	RE%		E (Volt)	EC (kWh/kg COD)
						Actual	Predict		
1	1	25	0.7	1	30	99	99.32	6.98	4.709
2	1	25	0.1	1	30	83.9	84.54	6.76	4.337
3	1	15	0.4	0	15	77	77.16	5.75	1.276
4	1	15	0.4	1	30	90.9	91.23	5.407	2.129
5	1	15	0.4	2	15	96.4	92.37	5.033	1.002

6	1	5	0.4	2	30	90	90.58	3.335	0.4513
7	1	15	0.4	1	30	91.1	91.23	5.34	2.113
8	1	5	0.1	1	30	65.57	64.05	3.43	0.552
9	1	15	0.4	2	45	98	96.64	4.99	2.798
10	1	15	0.7	1	45	99	100.09	4.87	2.960
11	1	25	0.4	1	15	92	90.89	6.77	2.092
12	1	15	0.7	1	15	90	92.73	5.102	1.014
13	1	5	0.4	1	15	74	75.56	3.43	0.249
14	1	15	0.7	0	30	98.87	95.57	5.41	2.066
15	1	15	0.4	0	45	84	86.83	5.91	3.679
16	1	15	0.1	1	45	78.71	77.75	5.53	3.452
17	1	25	0.4	2	30	97	98.09	6.3	4.107
18	1	5	0.4	0	30	71.56	72.25	3.747	0.595
19	1	25	0.4	1	45	98	95.86	6.67	6.084
20	1	5	0.4	1	45	84	84.53	3.714	0.794
21	1	15	0.1	0	30	67.11	65.54	5.74	2.67
22	1	15	0.4	1	30	91.7	91.23	5.44	2.149
23	1	15	0.7	2	30	99	99.99	4.97	4.295
24	1	5	0.7	1	30	95	93.16	3.29	0.398
25	1	15	0.1	2	30	83.4	86.13	4.88	2.003
26	1	15	0.1	1	15	70.5	71.18	4.98	1.136
27	1	25	0.4	0	30	90.2	91.4	7.15	4.49

It was observed that efficiency of COD removal is in the range of 65.57- 99.00%. The energy consumption is in the range of (0.249-6.084) Kwh/kg COD. It is clear that effect of $FeSO_4$ concentration on the efficiency of COD removal was the major as shown in the comparison between runs (1 and 2) where COD removal increased from 83.9 to 99% as $FeSO_4$ concentration increased from 0.1to 0.7mM at current density of 25mA/cm^2. At lower current density (5mA/cm^2), the effect of $FeSO_4$ concentration is more obvious as shown in comparison between runs (8 and 24) where COD removal increased from 65.57 to 95% as $FeSO_4$ concentration increased from 0.1to 0.7mM. Comparison between runs (1 and 24) showed that effect of current density is lower than the effect of $FeSO_4$ concentration where COD removal increased from 95 to 99% as current density increased from 5 to 25mA/cm^2. This comparison confirm that the process is controlled by Fenton reaction rather than electrodes reactions. However, increasing of current density would be enhanced the performance of Fenton reaction.

Minitab-17 software was used to analyze results of COD removal efficiency where an experimental relationship between COD removal efficiency and process parameters was obtained and formulated by the following quadratic model of the efficiency COD removal (RE%) in term of un-coded(real) units of process parameters:

$$RE\% = 10.07 + 2.339\,X1 + 98.8\,X2 + 20.32\,X3 + 0.985\,X4 - 0.0235\,(X1)^2 - 40.2\,(X2)^2 - 0.81\,(X3)^2 - 0.00966\,(X4)^2 - 1.194\,X1*X2 - 0.291\,X1*X3 - 0.00667\,X1*X4 - 13.47\,X2*X3 + 0.044\,X2*X4 - 0.09\,X3*X4 \quad (11)$$

Where RE% is the response, i.e. COD removal efficiency, and X1, X2, X3and X4 are current density, $FeSO_4$ concentration, NaCl concentration, and Time respectively. Whereas the variables X1X2, X1X3 ,X1X4,X2X3,X2X4,X3X4 represent the interaction effect of all the parameters of the model. $(X1)^2$, $(X2)^2$, $(X3)^2$ and $(X4)^2$ represent the measures of the main effect of variables current density, $FeSO_4$ concentration, NaCl concentration, and Time respectively.

Eq.(11) shows how the COD removal efficiency is influenced by the individual variables (linear and quadratic) or double interactions. Values of positive coefficients revealed that the COD removal efficiency increased with the increasing of the related factors of these coefficients within the tested range while values of negative coefficients revealed the opposite effect. As can be seen all parameters have a positive effect on COD removal efficiency. The results showed that effects of interactions are significant with a total contribution of (8.47%) from the model. The predicted values of the COD removal efficiency estimated from Eq.11 are also inserted in Table 4. The Box-Behnken design acceptability was recognized by using analysis of variance (ANOVA). For examine hypotheses on the factors of the model, ANOVA divides the total variation in a set of data into individual parts accompanied with specific sources of variation [49]. The acceptability of the model in ANOVA analysis is determined based on Fisher F-test and P-test. If the value of Fisher is large then most of the variation in the response can be illustrated by the regression

equation. P-value is used for evaluating whether F is large enough to recognize if the model is statistical significance. (90)% of the variability of the model could be clarified when a P-value lower than (0.05) [50].Table 5 illustrates ANOVA for the response surface model. In this table, the following terms were evaluated: percentage of contribution (Cr. %) , degree of freedom (DF), sum of the square (Seq. SS), adjusted sum of the square (Adj. SS), adjusted mean of the square (Adj. MS), P-value, and F-value. P-value of (0.0001) and F-value of (31.82) were obtained which elucidate that regression model is highly significance. The multiple correlation coefficient of the model was 97.38% conforming the regression is statistically significant and only (2.62) % of the total variations is not confirmed by the model. The adjusted multiple correlation coefficient (adj. R^2 = 94.32%) and the predicted multiple correlation coefficient (pred. R^2=84.93%) in this model were well-matched.

Results of ANOVA showed that $FeSO_4$ concentration has the main impact on the process with a contributions of 49.54% followed by current density with a contribution of (18.27%) and addition of NaCl with a contribution of 16.10%. Time has the miner effect on the process with a contribution of 4.99%. It can be seen that contribution of $FeSO_4$ concentration has the main effect on COD removal in the present work which means that the system is governed by reaction conditions in the bulk of solution i.e. the system is under bulk reaction control (reaction of ferrous ions with H_2O_2) [11]. The contribution of linear term is the main in the model with 88.91% followed by 2-way interaction with a contribution of 5.55% then the square term with contribution percent of 2.92%. The results showed that interaction of $FeSO_4$ concentration with NaCl concentration and $FeSO_4$ concentration with current density are significant. This is expected since these parameters effect on the electro-Fenton reactions.

Table 5
Analysis of variance for COD removal

Source	DOF	Seq SS	Cr.(%)	Adj SS	Adj MS	Fisher-Value	P-value
Model	14	2840.12	97.38	2840.12	202.87	31.82	0.001
Linear	4	2593.08	88.91	2593.08	648.27	101.68	0.001
(X1)	1	532.93	18.27	532.93	532.93	83.59	0.001
(X2)	1	1444.97	49.54	1444.97	1444.97	226.64	0.001
(X3)	1	469.50	16.10	469.50	469.50	73.64	0.001
(X4)	1	145.67	4.99	145.67	145.67	22.85	0.001
Square	4	85.10	2.92	85.10	21.28	3.34	0.047
X1*X1	1	7.03	0.24	29.38	29.38	4.61	0.053
X2*X2	1	52.81	1.81	69.83	69.83	10.95	0.006
X3*X3	1	0.04	0.001	3.48	3.48	0.55	0.474
X4*X4	1	25.22	0.86	25.22	25.22	3.96	0.070
2-Way Inter.	6	161.94	5.55	161.94	26.99	4.23	0.016
X1*X2	1	51.34	1.76	51.34	51.34	8.05	0.015
X1*X3	1	33.87	1.16	33.87	33.87	5.31	0.040
X1*X4	1	4.00	0.14	4.00	4.00	0.63	0.444
X2*X3	1	65.29	2.24	65.29	65.29	10.24	0.008
X2*X4	1	0.16	0.01	0.16	0.16	0.02	0.878
X3*X4	1	7.29	0.25	7.29	7.29	1.14	0.306
Error	12	76.51	2.62	76.51	6.38		
Lack-of-Fit	10	76.16	2.61	76.16	7.62		
Pure Error	2	0.35	0.01	0.35	0.17		
Total	26	2916.63	100.00				

Model summary	S	R^2	R^2 (adj.)	press	R^2 (pred.)
	2.525	97.38%	94.32%	439.466	84.93%

3.2 Effect of process variables on the COD removal efficiency

The interactive effect of the selected variables and their effect on the response was assessed via graphical representations of the statistical optimization using RSM. Figures (4-a, b) show the effect of the $FeSO_4$ concentration on the efficiency of COD removal for various values of current density (5-25 mA/cm^2) at constant NaCl conc. (1g/l) and time (30 min.). Figure 4-a represents the response surface plot while figure 4-b shows the corresponding contour plot. From surface plot, it is clear that, at current density (5 mA/cm^2), a sharply decreasing in COD removal efficiency occurs as the

$FeSO_4$ concentration decreased from 0.7 to 0.1 mM. At higher current density (25mA/cm^2), similar observation was found but with more sluggish. This behavior can be interpreted as Fe^{+2} improved the oxidizing power of H_2O_2 to degrade large molecules, therefor increasing concentration of Fe^{+2} results in more degradation of organic compounds in wastewater[11] . Previous studies showed that Fe^{+2} had a big impact on degrading big molecule in wastewater such as dyestuffs, in real dyeing wastewater [51]. At $FeSO_4$ concentration 0.1 mM, the results showed that the efficiency of COD removal is increased linearly with increasing of current density from 5 to 25 mA/cm^2. Similar observation was found when $FeSO_4$ concentration is 0.7 mM but with more sluggish. This behaviour of the effect of current density on the efficiency of COD removal is in agreement with previous work [52,53] and could be explained as the current is the driving force for the reduction of oxygen on the cathode surface leading to generating H_2O_2 hence, by increasing the current density, more generation of hydroxyl radicals would be occurred due to more reaction of H_2O_2 with ferrous ions. The corresponding contour plot confirms that value of the COD removal efficiency ≥95% lies in a small area in which the current density ranged between 8-25 mA/cm^2 and $FeSO_4$ concentration in the range (0.4-0.7 mM).

The impact of NaCl addition (concentration of NaCl) on the efficiency of COD removal for different current densities (5-25 mA/cm^2) at constant $FeSO_4$ concentration (0.4mM) and time (30 min.) is shown in Figures (5-a,b). The response surface plot (5-a) shows that COD removal efficiency is linearly increased with increasing of NaCl concentration at current density 5mA/cm^2. However, at high current density (25 mA/cm^2), COD removal efficiency slightly increased with increasing of NaCl concentration. The corresponding contour plot (5-b) confirms that value of the COD removal efficiency ≥95% lies in a small area in which the current density ranged between 12-25 mA/cm^2 and addition of NaCl at concentration between (1.0-2.0 g/l).

Figures (6-a,b) show the impact of time on the efficiency of COD removal for various values of current density (5-25 mA/cm^2) at constant $FeSO_4$ concentration (0.4mM) and NaCl conc. (1g/l). Figure 6-a shows that the COD removal efficiency is exponentially increased with increasing of time at low value of current density (5mA/cm^2). However no significant increase in COD removal efficiency occurred beyond 30 min. The same behavior was observed as the current density increased to 25 mA/cm^2 but with more sluggish. These results are in agreement with the results observed in the literature [54-57]. The results show that the reaction time has a positive effect on the progress of electro- Fenton process however by increasing the time its effect is decreased so after the optimum time, the efficiency of process does not essentially altered with time for this reason, the optimal response is achieved almost 2/3 of the total time as reported by previous works[55, 58]. The corresponding contour plot (6-b) confirms that value of the COD removal efficiency ≥95% lies in a small area in which the current density ranged between 20-25 mA/cm^{2}and times in range of 30-45 min. Therefore, application of RSM will lead to identify the possible optimum values of the studied parameters as well as its role in giving valuable information on interactions between the factors.

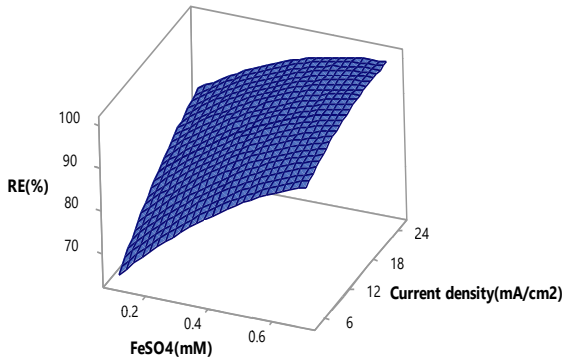

(a)

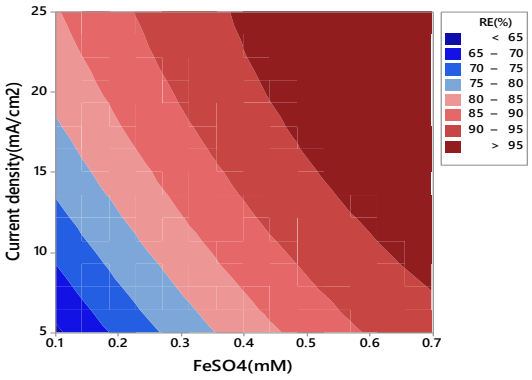

(b)

Figure 4. Response surface plot (a) and contour plot (b) for the impact of $FeSO_4$ concentration and current density on the COD removal efficiency (RE%)(Hold values: NaCl=1g/l, time =30 min)

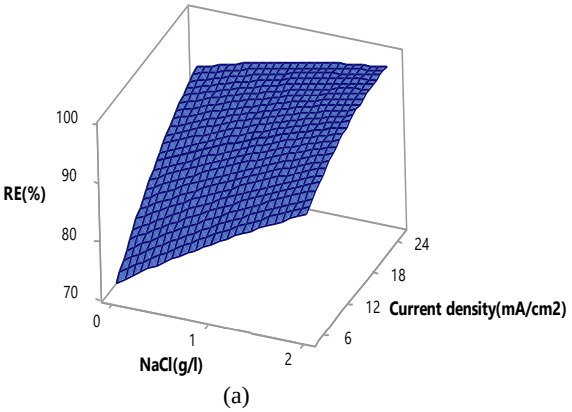

(a)

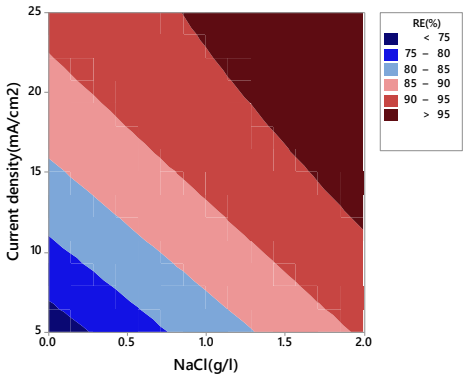

(b)

Figure 5. Response surface plot (a) and contour plot (b) showing the effect of NaCl concentration and current density on the COD removal efficiency(RE%) (Hold values: $FeSO_4$ concentration =0.4mM, time=30min).

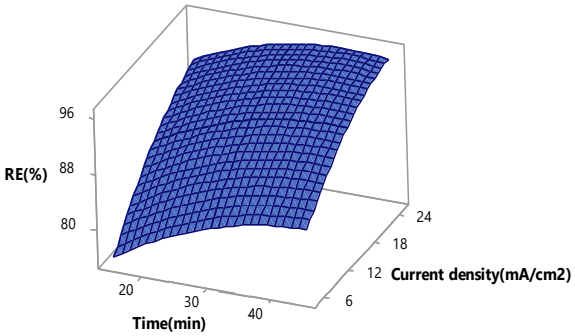

(a)

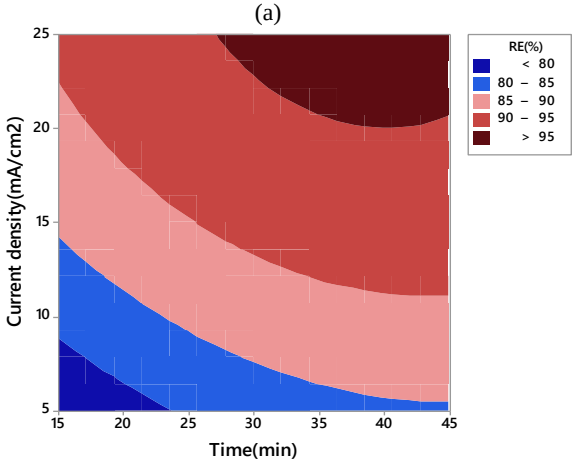

(b)

Figure 6. Response surface plot (a) and contour plot (b) showing the effect of time and current density on the COD removal efficiency(RE%) (Hold values: NaCl=1g/l, $FeSO_4$ concentration =0.4mM).

3.3 The optimization and confirmation test

For reducing energy losses for any electrochemical removal system, optimization of its process conditions is essential and should be achieved. For optimizing the system, many criteria were identified to accomplish the desired objective via maximizing the desirability function (D_F) through adjusting the weight or importance, which could change the features of an objective. The target fields for the variables have five options: maximize, objective, minimize, within the range, and none. The target of electrochemical removal of COD was selected as the 'maximum' with corresponding 'weight'1.0. The independent parameters studied in this work were recognized within the range of the designed levels (current: 5-25 mA/cm^2, $FeSO_4$ concentration: 0.1-0.7mM, NaCl: 0-2g/l and time: 15-45 min.). The lower limit value of the COD removal efficiency was assigned at 65.57%, while the upper limit value was assigned at 99%. The procedure of optimization was achieved under these boundaries and settings and the results are shown in Table 5 with the desirability function of (1). For their validation, two confirmative experiments were performed using the optimized parameters, the results are displayed in Table 7. After 45 min of the electrolysis, COD removal efficiency of 94.9% as average value was achieved at pH=3 which is in compactible with the range of the optimum value getting from optimization analysis with desirability function of (1) (Table 5). Therefore adopting Box–Behnken design in combined with desirability function is successful and efficient in optimizing COD removal using porous graphite anode. Table 7 shows a comparison between the properties of wastewater effluent and the treated effluent based on the present work. It can be seen that treated effluent has better properties and its properties are in agreement with the standard limits for discharging effluent (Table 1). COD removal efficiency of 95.9%, phenol removal efficiency of 92.8%, and turbidity removal efficiency of 95.05% base on the raw effluent properties were achieved in the present work confirming the activity of porous graphite electrodes in the electro-Fenton of wastewater generated from Al-Dewaniya petroleum refinery plant.

Table 5: Optimum of process parameters for maximum COD removal efficiency (RE%).

Response	Goal	Lower	Target	Upper	Weight	Importance
RE (%)	Maximum	65.57	Maximum	99	1	1

Solution:	Parameters			Results				
Current density (mA/cm^2)	FeSO4 (mM)	NaCl (g/l)	Time (min)	R E (%) Fit	D_F	SE Fit	95% CI	95% PI
25	0.7	0	43.8	101.08	1	3.70	(93.02; 109.13)	(91.32; 110.83)

Table 6. Confirmative value of the optimum COD removal efficiency:

Run	Current density (mA/cm^2)	$FeSO_4$ (mM)	NaCl (g/l)	Time (min)	E (Volt)	COD (ppm)		R E (%)		EC (Kwh/ kg COD)
						Initial	Final	Actual	Average	
1	25	0.7	0	45	7	567	34.5	93.9	94.9	8.626
2	25	0.7	0	45	7.3	560	23	95.9		8.921

Table 7. Comparison between the wastewater effluent and the treated effluent**:**

Parameter / Effluent	COD (ppm)	Phenol (ppm)	Turbidity (NTU)	$SO4^{-2}$ (ppm)	Cl^- (g/l)
Raw effluent	560	0.1366	25.07	8.835	1.4
Treated effluent	23(96%)	0.0098 (92.8%)	1.24 (95.05%)	619	1.081

3.4 Comparison with previous works

The optimum conditions revealed that the electro-Fenton process can be applied for treatment of Al-Dewaniya petroleum refinery using porous graphite electrodes. By starting from an initial COD (560 ppm) , COD removal efficiency of 96% could be achieved at the end of an electrolysis time of 45 min. In this case an energy consumption of 8.921kWh/kg COD is required. In the literature, few studies were achieved for treatment of petroleum refinery wastewater using electro-Fenton process [8, -57]. In Table 7, we have given a comparison between the present work with the others related to petroleum refinery wastewater degradation by electro-Fenton process using different types of electrode under various conditions.

Table 9. Comparison of petroleum refinery wastewater degradation study by electro-Fenton process using different Type of electrodes with literature under various conditions

Electrode type	COD Ppm	Current density mA/cm^2	Time (min)	COD RE (%)	Ref.
Aluminum	1400–1700	68.65	78.97	51.23	[8]
Iron		59.7	73.19	66.85	
ferrous electrodes	1,895	60.89	62.05	80.13	[53]
ferrous electrodes	1,895	52.5	90	82.55	[54]
Iron electrodes	1500	57.01	86.33	75.52	[56]
Aluminum Oxide Anode Aluminum cathode	1500	69.57	89.51	65.03	[57]
Porous graphite plates + Fe particles	4753	12Volt	60	83.65	[58]
Porous Graphite	560	25	45	96	This work

It can be seen that the results of the present work are better than other mentioned works that used other different electrodes in term of higher COD removal, lower electrolysis time, and lower applied current density. This probably due to the high surface area of porous graphite that leads to liberation of more quantity of H_2O_2 on the cathode surface hence more reaction of H_2O_2 with ferrous ions leading to more removal of organic pollutants in wastewater. Besides using porous graphite as anode and cathode materials make the process more efficient for treatment of petroleum refinery as mentioned by Yan et

al.[57] and for other types of wastewaters as mentioned by previous studies [16, 36].

4. Conclusions

The present research focused on investigating the impact of many operating factors such as current density, $FeSO_4$ concentration, NaCl concentration, and time on the COD removal in the treatment of Al-Dewaniya petroleum refinery wastewater using electro-Fenton process on porous graphite electrodes and adopting Box-Behnken design as an optimization method. The experimental data were fitted to a second-order polynomial equation which was utilized for optimization of operating parameters. The optimum conditions were current density of 25 A/cm^2, $FeSO_4$ concentration of 0.7mM, and electrolysis time of 45 min with no addition of NaCl, where COD removal efficiency of 96%, with energy consumption of 8.921KWh/Kg COD were obtained. Results show that $FeSO_4$ concentration has the main effect on COD removal in the present work which means that the system is governed by reaction conditions in the bulk of solution not upon the reactions on the surface of electrodes (anodic and cathodic reactions). This was in agreement with most mechanisms of electro-Fenton reactions reported in the literature. The optimization results showed that addition of NaCl is not required at the optimum conditions in spite of this parameter was considered as one of the main factors affecting on the process. The reason is that, at higher current density, the system is controlled totally by Fenton reaction with a minor contribution of chlorine reaction with water.

Acknowledgment

The authors wish to thank all staff of Chemical Engineering Department, College of Engineering- University of Al-Qadisiyah for their technical assistance for achieving this research.

References

[1] P. Mijaylova, "Water Management in the Petroleum Refining Industry," *Water Conserv.*, 2011, doi: 10.5772/31018.

[2] A. Coelho, A. V Castro, M. Dezotti, and G. L. Sant'Anna Jr, "Treatment of petroleum refinery sourwater by advanced oxidation processes," *J. Hazard. Mater.*, vol. 137, no. 1, pp. 178–184, 2006.

[3] R. O. Ackermann *et al.*, *Pollution prevention and abatement handbook 1998: toward cleaner production*, no. 19128. The world bank, 1999.

[4] B. Mrayyan and M. N. Battikhi, "Biodegradation of total organic carbons (TOC) in Jordanian petroleum sludge," *J. Hazard. Mater.*, vol. 120, no. 1–3, pp. 127–134, 2005.

[5] A. Roudi, S. Chelliapan, H. Kamyab, M. F. Md Din, and S. Krishnan, "Removal of COD from landfill leachate by Predication and Evaluation of Multiple Linear Regression (MLR) Model and Fenton process," *Egypt. J. Chem.*, vol. 62, no. 7, pp. 1207–1218, 2019.

[6] J. Saien and H. Nejati, "Enhanced photocatalytic degradation of pollutants in petroleum refinery wastewater under mild conditions," *J. Hazard. Mater.*, vol. 148, no. 1–2, pp. 491–495, 2007.

[7] Y. Yavuz and A. S. Koparal, "Electrochemical oxidation of phenol in a parallel plate reactor using ruthenium mixed metal oxide electrode," *J. Hazard. Mater.*, vol. 136, no. 2, pp. 296–302, 2006.

[8] R. Davarnejad, M. Mohammadi, and A. F. Ismail, "Petrochemical wastewater treatment by electro-Fenton process using aluminum and iron electrodes: Statistical comparison," *J. Water Process Eng.*, vol. 3, pp. 18–25, 2014.

[9] P. V Nidheesh and R. Gandhimathi, "Trends in electro-Fenton process for water and wastewater treatment: an overview," *Desalination*, vol. 299, pp. 1–15, 2012.

[10] N. Wang, T. Zheng, G. Zhang, and P. Wang, "A review on Fenton-like processes for organic wastewater treatment," *J. Environ. Chem. Eng.*, vol. 4, no. 1, pp. 762–787, 2016.

[11] H. He and Z. Zhou, "Electro-Fenton process for water and wastewater treatment," *Crit. Rev. Environ. Sci. Technol.*, vol. 47, no. 21, pp. 2100–2131, 2017.

[12] L. Ma, M. Zhou, G. Ren, W. Yang, and L. Liang, "A highly energy-efficient flow-through electro-Fenton process for organic pollutants degradation," *Electrochim. Acta*, vol. 200, pp. 222–230, 2016.

[13] M. H. El-Awady, I. Abdelfattah, and A. A. El-Magd, "Reliable treatment of petroleum processing wastewater using dissolved air flotation in combination with advanced oxidation process," *Egypt. J. Chem.*, vol. 58, no. 6, pp. 609–624, 2015.

[14] A. Babuponnusami and K. Muthukumar, "A review on Fenton and improvements to the Fenton process for wastewater treatment," *J. Environ. Chem. Eng.*, vol. 2, no. 1, pp. 557–572, 2014.

[15] Y. Liu, J. Xie, C. N. Ong, C. D. Vecitis, and

Z. Zhou, "Electrochemical wastewater treatment with carbon nanotube filters coupled with in situ generated H 2 O 2," *Environ. Sci. Water Res. Technol.*, vol. 1, no. 6, pp. 769–778, 2015.

[16] P. V Nidheesh and R. Gandhimathi, "Removal of Rhodamine B from aqueous solution using graphite–graphite electro-Fenton system, Desalin," *Water Treat*, 2013.

[17] L. Ciríaco, C. Anjo, J. Correia, M. J. Pacheco, and A. Lopes, "Electrochemical degradation of ibuprofen on Ti/Pt/PbO2 and Si/BDD electrodes," *Electrochim. Acta*, vol. 54, no. 5, pp. 1464–1472, 2009.

[18] C. Flox, C. Arias, E. Brillas, A. Savall, and K. Groenen-Serrano, "Electrochemical incineration of cresols: a comparative study between PbO2 and boron-doped diamond anodes," *Chemosphere*, vol. 74, no. 10, pp. 1340–1347, 2009.

[19] M. A. Rodrigo, P. Cañizares, A. Sánchez-Carretero, and C. Sáez, "Use of conductive-diamond electrochemical oxidation for wastewater treatment," *Catal. Today*, vol. 151, no. 1–2, pp. 173–177, 2010.

[20] E. Brillas, S. Garcia-Segura, M. Skoumal, and C. Arias, "Electrochemical incineration of diclofenac in neutral aqueous medium by anodic oxidation using Pt and boron-doped diamond anodes," *Chemosphere*, vol. 79, no. 6, pp. 605–612, 2010.

[21] H. Zhang, C. Fei, D. Zhang, and F. Tang, "Degradation of 4-nitrophenol in aqueous medium by electro-Fenton method," *J. Hazard. Mater.*, vol. 145, no. 1–2, pp. 227–232, 2007.

[22] J. Casado, J. Fornaguera, and M. I. Galán, "Mineralization of aromatics in water by sunlight-assisted electro-Fenton technology in a pilot reactor," *Environ. Sci. Technol.*, vol. 39, no. 6, pp. 1843–1847, 2005.

[23] J. Y. Choi, Y.-J. Lee, J. Shin, and J.-W. Yang, "Anodic oxidation of 1, 4-dioxane on boron-doped diamond electrodes for wastewater treatment," *J. Hazard. Mater.*, vol. 179, no. 1–3, pp. 762–768, 2010.

[24] M. S. Çelebi, N. Oturan, H. Zazou, M. Hamdani, and M. A. Oturan, "Electrochemical oxidation of carbaryl on platinum and boron-doped diamond anodes using electro-Fenton technology," *Sep. Purif. Technol.*, vol. 156, pp. 996–1002, 2015.

[25] O. García, E. Isarain-Chávez, S. Garcia-Segura, E. Brillas, and J. M. Peralta-Hernández, "Degradation of 2, 4-dichlorophenoxyacetic acid by electro-oxidation and electro-Fenton/BDD processes using a pre-pilot plant," *Electrocatalysis*, vol. 4, no. 4, pp. 224–234, 2013.

[26] G. Pliego, J. A. Zazo, P. Garcia-Muñoz, M. Munoz, J. A. Casas, and J. J. Rodriguez, "Trends in the intensification of the Fenton process for wastewater treatment: an overview," *Crit. Rev. Environ. Sci. Technol.*, vol. 45, no. 24, pp. 2611–2692, 2015.

[27] Y.-H. Huang, Y.-F. Huang, P.-S. Chang, and C.-Y. Chen, "Comparative study of oxidation of dye-Reactive Black B by different advanced oxidation processes: Fenton, electro-Fenton and photo-Fenton," *J. Hazard. Mater.*, vol. 154, no. 1–3, pp. 655–662, 2008.

[28] X.-Q. Wang, C.-P. Liu, Y. Yuan, and F. Li, "Arsenite oxidation and removal driven by a bio-electro-Fenton process under neutral pH conditions," *J. Hazard. Mater.*, vol. 275, pp. 200–209, 2014.

[29] P. V Nidheesh, R. Gandhimathi, S. Velmathi, and N. S. Sanjini, "Magnetite as a heterogeneous electro Fenton catalyst for the removal of Rhodamine B from aqueous solution," *Rsc Adv.*, vol. 4, no. 11, pp. 5698–5708, 2014.

[30] G. Gao, Q. Zhang, Z. Hao, and C. D. Vecitis, "Carbon nanotube membrane stack for flow-through sequential regenerative electro-Fenton," *Environ. Sci. Technol.*, vol. 49, no. 4, pp. 2375–2383, 2015.

[31] N. Daneshvar, S. Aber, V. Vatanpour, and M. H. Rasoulifard, "Electro-Fenton treatment of dye solution containing Orange II: Influence of operational parameters," *J. Electroanal. Chem.*, vol. 615, no. 2, pp. 165–174, 2008.

[32] M. M. Ghoneim, H. S. El-Desoky, and N. M. Zidan, "Electro-Fenton oxidation of Sunset Yellow FCF azo-dye in aqueous solutions," *Desalination*, vol. 274, no. 1–3, pp. 22–30, 2011.

[33] B. B. Wang, M. H. Cao, Z. J. Tan, L. L. Wang, S. H. Yuan, and J. Chen, "Photochemical decomposition of

perfluorodecanoic acid in aqueous solution with VUV light irradiation," *J. Hazard. Mater.*, vol. 181, no. 1–3, pp. 187–192, 2010.

[34] H. Liu, C. Wang, X. Li, X. Xuan, C. Jiang, and H. Cui, "A novel electro-Fenton process for water treatment: reaction-controlled pH adjustment and performance assessment," *Environ. Sci. Technol.*, vol. 41, no. 8, pp. 2937–2942, 2007.

[35] J. Li, D. Song, K. Du, Z. Wang, and C. Zhao, "Performance of graphite felt as a cathode and anode in the electro-Fenton process," *RSC Adv.*, vol. 9, no. 66, pp. 38345–38354, 2019.

[36] P. V Nidheesh, R. Gandhimathi, and N. S. Sanjini, "NaHCO3 enhanced Rhodamine B removal from aqueous solution by graphite–graphite electro Fenton system," *Sep. Purif. Technol.*, vol. 132, pp. 568–576, 2014.

[37] S. J. George, R. Gandhimathi, P. V. Nidheesh, and S. T. Ramesh, "Electro-Fenton method oxidation of salicylic acid in aqueous solution with graphite electrodes," *Environ. Eng. Sci.*, vol. 30, no. 12, pp. 750–756, 2013.

[38] S. Liu *et al.*, "Degradation of organic pollutants by a Co 3 O 4-graphite composite electrode in an electro-Fenton-like system," *Chinese Sci. Bull.*, vol. 58, no. 19, pp. 2340–2346, 2013.

[39] C. Yang and D. Wang, "The optimal factors of electro-Fenton process to decolorization the azo ddye methyl orange in aqueous medium," in *2011 International Conference on Remote Sensing, Environment and Transportation Engineering*, 2011, pp. 3682–3685.

[40] R. B. A. Souza and L. A. M. Ruotolo, "ESouza, R. B. A., & Ruotolo, L. A. M. (2013). Electrochemical treatment of oil refinery effluent using boron-doped diamond anodes. Journal of Environmental Chemical Engineering, 1(3), 544–551.lectrochemical treatment of oil refinery effluent using boron-d," *J. Environ. Chem. Eng.*, vol. 1, no. 3, pp. 544–551, 2013.

[41] E. Marlina, "Electro-Fenton for Industrial Wastewater Treatment: A Review," in *E3S Web of Conferences*, 2019, vol. 125, p. 3003.

[42] L. Nova *et al.*, "Advanced oxidation processes and their application in the petroleum industry: a review," *Brazilian J. Pet. Gas*, vol. 2, no. 3, pp. 122–142, 2009.

[43] N. Balasubramanian, "Treatment of petroleum refinery effluent using electrochemical techniques," 2013.

[44] M. A. Bezerra, R. E. Santelli, E. P. Oliveira, L. S. Villar, and L. A. Escaleira, "Response surface methodology (RSM) as a tool for optimization in analytical chemistry," *Talanta*, vol. 76, no. 5, pp. 965–977, 2008.

[45] M. Evans, *Optimisation of manufacturing processes: a response surface approach*, vol. 791. Maney Pub, 2003.

[46] Y.-D. Chen, W.-Q. Chen, B. Huang, and M.-J. Huang, "Process optimization of K2C2O4-activated carbon from kenaf core using Box–Behnken design," *Chem. Eng. Res. Des.*, vol. 91, no. 9, pp. 1783–1789, 2013.

[47] K. Yetilmezsoy, S. Demirel, and R. J. Vanderbei, "Response surface modeling of Pb (II) removal from aqueous solution by Pistacia vera L.: Box–Behnken experimental design," *J. Hazard. Mater.*, vol. 171, no. 1–3, pp. 551–562, 2009.

[48] Z. Q. Li, C. J. Lu, Z. P. Xia, Y. Zhou, and Z. Luo, "X-ray diffraction patterns of graphite and turbostratic carbon," *Carbon N. Y.*, vol. 45, no. 8, pp. 1686–1695, 2007.

[49] L. Huiping, Z. Guoqun, N. Shanting, and L. Yiguo, "Technologic parameter optimization of gas quenching process using response surface method," *Comput. Mater. Sci.*, vol. 38, no. 4, pp. 561–570, 2007.

[50] J. Segurola, N. S. Allen, M. Edge, and A. Mc Mahon, "Design of eutectic photoinitiator blends for UV/visible curable acrylated printing inks and coatings," *Prog. Org. Coatings*, vol. 37, no. 1–2, pp. 23–37, 1999.

[51] C.-T. Wang, W.-L. Chou, M.-H. Chung, and Y.-M. Kuo, "COD removal from real dyeing wastewater by electro-Fenton technology using an activated carbon fiber cathode," *Desalination*, vol. 253, no. 1–3, pp. 129–134, 2010.

[52] A. Sahraei, "Wastewater treatment obtained from the Imam Khomein's refinery using electro-Fenton technique," *Arak Univ.*, 2013.

[53] R. Davarnejad and A. Sahraei, "Industrial wastewater treatment using an electrochemical technique: an optimized

process," *Desalin. Water Treat.*, vol. 57, no. 21, pp. 9622–9634, 2016.

[54] R. Davarnejad, M. Pirhadi, M. Mohammadi, and S. Arpanahzadeh, "Numerical analysis of petroleum refinery wastewater treatment using electro-Fenton process," *Chem. Prod. Process Model.*, vol. 10, no. 1, pp. 11–16, 2015.

[55] M. Panizza and M. A. Oturan, "Degradation of Alizarin Red by electro-Fenton process using a graphite-felt cathode," *Electrochim. Acta*, vol. 56, no. 20, pp. 7084–7087, 2011.

[56] H. FathinejadJirandehi, M. Adimi, and M. Mohebbizadeh, "Petrochemical wastewater treatment by modified electro-Fenton process with nano iron particles," *J. Part. Sci. Technol.*, vol. 1, no. 4, pp. 215–223, 2015.

[57] M. Adimi, M. Mohammadpour, and H. Fathinejadjirandehi, "Treatment of petrochemical wastewater by modified electro-fenton method with nano porous aluminum electrode," *J. Water Environ. Nanotechnol.*, vol. 2, no. 3, pp. 186–194, 2017.

[58] L. Yan *et al.*, "Comparative study of different electrochemical methods for petroleum refinery wastewater treatment," *Desalination*, vol. 341, pp. 87–93, 2014.